



Università degli Studi Mediterranea di Reggio Calabria
Archivio Istituzionale dei prodotti della ricerca

Computer vision for automatic quality inspection of dried figs (*Ficus carica* L.) in real-time

This is the peer reviewed version of the following article:

Original

Computer vision for automatic quality inspection of dried figs (*Ficus carica* L.) in real-time / Benalia, S., Cubero, S., Prats-Montalbán, J.M., Bernardi, B., Zimbalatti, G., Blasco, J.. - In: COMPUTERS AND ELECTRONICS IN AGRICULTURE. - ISSN 0168-1699. - 120:(2016), pp. 17-25. [10.1016/j.compag.2015.11.002]

Availability:

This version is available at: <https://hdl.handle.net/20.500.12318/3534> since: 2020-11-28T12:37:09Z

Published

DOI: <http://doi.org/10.1016/j.compag.2015.11.002>

The final published version is available online at: <https://www.sciencedirect.com>.

Terms of use:

The terms and conditions for the reuse of this version of the manuscript are specified in the publishing policy. For all terms of use and more information see the publisher's website

Publisher copyright

This item was downloaded from IRIS Università Mediterranea di Reggio Calabria (<https://iris.unirc.it/>) When citing, please refer to the published version.

(Article begins on next page)

This is the peer reviewed version of the following article [Benalia, S., Cubero, S., Prats-montalbán, J. M., Bernardi, B., Zimbalatti, G., Blasco, J. (2016). Computer vision for automatic quality inspection of dried figs (*Ficus carica* L .) in real-time. *Computers and Electronics in Agriculture*, 120, 17–25], which has been published in final [<https://doi:10.1016/j.compag.2015.11.002>]. The terms and conditions for the reuse of this version of the manuscript are specified in the publishing policy. For all terms of use and more information see the publisher's website.

1 **Computer vision for automatic quality inspection of dried Figs (*Ficus carica***
2 **L.) in real-time**

3 Souraya Benalia^a, Sergio Cubero^b, José Manuel Prats-Montalbán^c, Bruno Bernardi^{a*},
4 Giuseppe Zimbalatti^a, José Blasco^b

5 ^a *Dipartimento di Agraria. Università degli Studi Mediterranea di Reggio Calabria, Loc. Feo*
6 *di Vito, 89122 Reggio Calabria, Italy, e-mail: soraya.benalia@unirc.it,*
7 *bruno.bernardi@unirc.it, gzimbalatti@unirc.it*

8 ^b *Centro de Agroingeniería. Instituto Valenciano de Investigaciones Agrarias (IVIA), Cra.*
9 *Moncada-Naquera Km 5, Moncada, Spain, e-mail: jblasco.ivia@gmail.com,*
10 *cubero_ser@gva.es*

11 ^c *Departamento de Estadística e Investigación Operativa. Universitat Politècnica de*
12 *València, Camino de Vera s/n, 46022 Valencia, Spain, , e-mail: jopraron@eio.upv.es*

13 **ABSTRACT**

14 This work reports the development of automated systems based on computer vision to
15 improve the quality control and sorting of dried figs of Cosenza (protected denomination of
16 origin) focusing on two research issues. The first was based on qualitative discrimination of
17 figs through colour assessment comparing the analysis of colour images obtained using a
18 digital camera with those obtained according to conventional instrumental methods, i.e.
19 colourimetry currently done in laboratories. Data were expressed in terms of CIE XYZ,
20 CIELAB and HunterLab colour spaces, as well as the browning index measurement of each
21 fruit, and then, analysed using PCA and PLS-DA based methods. The results showed that
22 both chroma meter and image analysis allowed a complete distinction between high quality
23 and deteriorated figs, according to colour attributes. The second research issue had the
24 purpose of developing image processing algorithms to achieve real-time sorting of figs using

25 an experimental prototype based on machine vision, simulating an industrial application. An
26 extremely high 99.5% of deteriorated figs were classified correctly as well as 89.0% of light
27 coloured good quality figs. A lower percentage was obtained for dark good quality figs but
28 results were acceptable since the most of the confusion was among the two classes of good
29 product.

30 **Keywords:** fig; image analysis; computer vision; quality; colour; post-harvest processing

31 **1 INTRODUCTION**

32 The growing attention of consumers towards regional and local products and the relationship
33 these products have with their place of origin represents an interesting opportunity for
34 agricultural and rural development. The promotion of these high quality food products, which
35 can contribute considerably to rural development and agricultural diversification, could be
36 realized through designations of origin and geographical indications labels (European
37 Commission, 1996; De Luca et al., 2015). The designation of the protected denomination of
38 origin (PDO) 'Fichi di Cosenza DOP' (European Commission, 2011) exclusively regards
39 naturally dried fruits of the domestic fig "*Ficus carica sativa*" (*domestica* L.) belonging to the
40 variety 'Dottato' or 'Ottato', and presenting specific physical, chemical and organoleptic
41 features.

42 Very nutritional and healthy, dried figs constitute a popular food for local populations of the
43 Mediterranean area because of their content in sugars, mainly fructose and glucose, in
44 essential amino-acids, in carotene (vitamin A), thiamine (vitamin B1), riboflavin (vitamin
45 B2), ascorbic acid (vitamin C), and minerals such as K, P, Fe, Mg, Ca and Cu. They represent
46 an important source of fibre, and their high content in phenolic compounds strongly
47 contribute to their definition as functional fruits (Hatano et al., 2008; Farahnaky et al., 2009;
48 Vallejo et al., 2012). Nevertheless, this strategic cultivation often remains marginalized in

49 many rural areas, as reported by IPGRI and CIHEAM (2003), whereas it could contribute
50 significantly to their sustainable development. According to FAOSTAT (www.faostat.org),
51 fig production in Italy was 11,520 tons in 2013. In the same year, according to Istat data
52 (National Institute of Statistics – Italy), Calabria (Southern Italy) is second only to Campania
53 (Southern Italy), both in terms of cultivated area (474 ha) and production with 2,839 tons,
54 corresponding to 24% of the national total. In Calabria, fig cultivation is principally located in
55 the province of Cosenza, where the widest-grown cultivar is the ‘Dottato’.

56 Consumer expectations and requirements lead the agro-food industries to increase the
57 marketed product quality, extend its shelf life, and reduce the environmental impact.

58 However, the intrinsic biological variability between individual fruit and vegetable products
59 make it impossible for analytical destructive methods to ensure that each individual fruit
60 meets the high quality standards that constitute a fundamental criterion for a competitive
61 place in a global market. Dried figs should reach the minimum quality requirements
62 established by UNECE (United Nations, 2014). They should be ‘intact, sound, clean,
63 sufficiently developed, free from living pests and any of their damages, free from blemishes,
64 areas of discolouration, free from mould filaments, free of fermentation, free of abnormal
65 external moisture and free of foreign smell and/or taste except for a slight salty taste’.

66 Nowadays, the quality sorting of dried figs is carried out manually by experienced operators,
67 who are usually located on both sides of conveyors belts or rollers transporting fruits to be
68 sorted, but visual methods are slow, subjective and do not guarantee the quality of the whole
69 production. Hence, the agro-food industry has to implement new technologies that provide
70 rapid and reliable results, at the same time boosting product value along the entire supply
71 chain.

72 Consumer willingness to purchase often depends on the appearance of the product, which
73 may also influence the expectations relating to the organoleptic properties, and therefore

74 consumer behaviour. Colour perception is subjective and can be considered as an indicator of
75 freshness or maturity (Valadez-Blanco et al., 2007). Different physical systems have been
76 developed to avoid this subjectivity for colour analysis, which may be evaluated with visual
77 and/or instrumental procedures (González-Miret et al., 2007). Conventional instruments
78 analyse only a small part of the sample, and therefore are not appropriate for food that often
79 presents a heterogenic surface. As a consequence, artificial vision systems have been
80 developed in recent years in order to overcome this problem and to make colour analysis
81 more exhaustive and meticulous including the total surface of the product while carrying out
82 post-harvest operations (Kang & Sabarez, 2009). In this sense, non-destructive technologies
83 for foodstuff quality assessment such as machine vision systems constitute a promising tool
84 for quality control as well as product inspection, sorting and grading (Gómez-Sanchis et al.,
85 2013; Pallottino et al., 2013a & 2013b; Benalia et al., 2015). Indeed, images are both a large
86 data set and a visible entity that can be interpreted at the same time (Grahn & Geladi, 2007).
87 Recent progress in image acquisition techniques allows areas of millions of pixels to be
88 analysed using sophisticated systems (Martin et al., 2007).

89 Even though numerous studies have considered digital imaging for the various aspects of food
90 colour assessment in recent years (Mendoza et al., 2006; Kang & Sabarez, 2009; Menesatti et
91 al., 2009), they are still at an experimental scale. They certainly need to be optimized for
92 large-scale implementation in agro-food industries due to the complexity of such structures.
93 Computer vision systems developed to work at an industrial scale are far more complex than
94 those which acquire images of static fruit using still digital cameras. The fruit is in movement
95 and randomly oriented, the image acquisition has to be synchronised with the advance of the
96 fruit and the decision resulting from the image processing must be provided in real time to
97 deliver the fruit to the proper quality outlet. However if optimized for large scale
98 implantation, they are of great interest because of the advantages they present: mainly,

99 rapidness, effectiveness, accuracy and objectiveness; moreover, they are non destructive, do
100 not need sample treatment, and are able to assess the whole area of the product despite uneven
101 features present (Cubero et al.2011). Therefore, they allow cost and labour savings, especially
102 when used in automated processes.

103 The present work deals with the assessment of dried fig skin colour comparing two analytical
104 methods: image analyses and conventional colourimetry, analyzing PDO certified dried figs
105 ‘Fichi di Cosenza’, as well as deteriorated ones. Furthermore, automated sorting of figs using
106 an experimental prototype based on machine vision systems was developed in order to
107 confirm the obtained results and simulate post-harvest processing at an industrial scale.

108 **2 MATERIALS AND METHODS**

109 **2.1. Dried fig colour assessment**

110 Two groups of dried figs belonging to the variety ‘Dottato’ were chosen for trials. The first
111 group consisted of dried figs of excellent quality harvested during the 2012 season, provided
112 by the Consortium of ‘Fichi di Cosenza DOP’ (European Commission, 2011) in Southern
113 Italy. The second group, however, comprised purchased fruits of the same variety ‘Dottato’,
114 from the previous season, which showed a certain quality loss due to major sugar
115 crystallization, as well as to fungal and insect infestations.

116 Fig skin colour was first measured by means of the chroma meter CR-400 (Minolta Co.,
117 Osaka, Japan), using the CIE illuminant D65 and the 10° observer standard. The instrument
118 was calibrated using a white tile reference ($L^* = 97.59$, $a^* = -0.05$, $b^* = 1.65$). L^* value
119 indicates lightness when it is equal to 100, or darkness if it is equal to 0. However, a^* value
120 represents the red (positive value) or green (negative value); and b^* value constitutes the
121 yellow (positive value) or blue (negative value) (Rodov et al., 2012). Each fruit with a mean
122 of three measurements in different zones represented a replicate.

123 After the chroma meter measurements, image acquisition of each fig was performed with a
124 digital camera Canon EOS 550D, which captured images with a size of 2592 x 1728 pixels
125 and a resolution of 0.06 mm/pixel. Lighting was provided by eight fluorescent tubes
126 (BIOLUX 18 W/965, 6500 K, OSRAM, Germany) placed on the four sides of a square
127 inspection chamber in a 0°/45° configuration. The camera was connected to a computer, and
128 image analysis was performed according to a software specially developed for this purpose at
129 the Laboratory of Artificial Vision for Agriculture (IVIA-Spain), which separates the objects
130 (figs) from the background using the RGB.R value, and then converts the obtained R, G, B
131 values from the pixels selected as figs into HunterLab space. The first step consists in the
132 conversion of RGB values to CIE XYZ values, then, from CIE XYZ to L, a, b coordinates as
133 described by Vidal et al., (2013) and to L^*, a^*, b^* coordinates attending the equations in
134 HunterLab (2008), in both cases assuming a D65 (6500 K) illuminant and a 10° observer.
135 Since RGB colour model is device dependent (Menesatti et al., 2012), a previous calibration
136 step was done consisting in the comparison of the colour of each patch of a digital colour
137 checker (Digital ColorChecker SG Card, X-Rite Inc, USA) acquired using the chroma meter
138 and the camera. The colours were then converted from RGB to CIELAB and a linear
139 regression was done between both series of values giving a $R^2 > 0.98$ for the three L^*, a^* and
140 b^* components. Hence, it was considered that the camera provided accurate colours.

141 ***2.1.2. Data analysis***

142 Data obtained from both conventional colourimetry and image analysis were then expressed
143 in terms of $XYZ.X, XYZ.Y, XYZ.Z, L^*, a^*, b^*, L, a, b$ coordinates, and the ratios $L/a, L^*/a^*$ in
144 order to look for those variables that permit the best separation between both groups since it
145 was the first time that such analyses had been done on dried figs. In addition, the browning
146 index (BI), which is considered to be an important parameter where enzymatic or non-

147 enzymatic browning processes occur (Mohammad et al., 2008), was also calculated and
148 considered in the model (eq. 1, Palou et al., 1999).

$$149 \quad BI = \frac{100(x - 0.31)}{0.172} \quad (\text{eq. 1})$$

150 where:

$$151 \quad x = \frac{a + 1.75L}{5.645L + a - 3.012b}$$

152 At the end of the trial, a total of 26 parameters (variables) were obtained and statistically
153 analyzed according to principal component analysis (PCA) and partial least squares -
154 discriminant analysis (PLS-DA), using SIMCA-P v13 (MKS Umetrics AB, Sweden). In order
155 to compress and interpret the internal relationships between variables, and at the same time
156 check whether some of these are able to separate the two analyzed classes (deteriorated and
157 not deteriorated figs), principal component analysis PCA (Jackson, 1991) was applied. PCA is
158 a projection method of the original variables onto new ones, called latent variables,
159 orthogonal and arranged according to their explained variance. This is carried out expressing
160 a matrix X as:

$$161 \quad X = TP^T + E \quad (\text{eq. 2})$$

162 where T is the score matrix, P is the loading matrix and E is the residual matrix for X . This
163 makes it possible to determine the general pattern of any process, and the relevant variables
164 that rule it.

165 However, PCA does not necessarily search for those variables that better discriminate
166 between classes, but only for those gathering the highest variance in the data. Thus, when
167 aiming to separate, another latent-based multivariate projection model, such as PLS-DA
168 (Sjöström et al., 1986) is a more sensitive technique to apply. PLS (Geladi & Kowalski, 1986)
169 models the data through the use of eq. 2 and the following expressions:

170 $T=XW^*=XWP^TW$ (eq. 3)

171 $Y=TC^T+F$ (eq. 4)

172 where T is the score matrix, P the loading matrix for X , C the loading matrix for Y , W and W^*
173 weighting matrices, and F the residual matrix for Y .

174 In the case of PLS-DA, Y is built from as many dummy variables as classes we have to
175 separate. A dummy variable is a binary variable formed by 1's and 0's, the former linked to
176 the class the dummy variable is related to, and zeros to the rest of the observations. Hence, the
177 PLS-DA looks for those internal directions that best separate the classes of interest, also
178 trying to explain X reasonably.

179 This way, it is possible to compute, from any matrix X , the prediction of Y as:

180 $Y_{pred} = XB_{PLS}=TQ^T=XW(P^TW)^{-1}Q^T$ (eq. 5)

181 where

182 $B_{PLS}=XW(P^TW)^{-1}Q^T$

183 When applied to images, these techniques belong to Multivariate Image Analyses, MIA
184 (Prats-Montalbán et al., 2011). Together they make up the most suitable analytical tools for
185 the trials that were carried out, taking into account that each sample was considered regarding
186 its 26 variables.

187 **2.2. In-line dried fig sorting**

188 Due to the high complexity of handling small fruit and the relatively small market in
189 comparison to other fresh fruit, there are not commercial electronic sorters of dried figs to
190 separate them into qualities. Hence, there is a need to develop such a sorter. For this purpose,
191 automated sorting trials based on a computer vision system were performed using an
192 experimental prototype, developed at the Laboratory of Artificial Vision for Agriculture

193 (IVIA-Spain). It was originally designed for mandarin orange segment and pomegranate aril
194 in-line sorting (Blasco et al., 2009a; Blasco et al., 2009b) and subsequently adapted for the
195 sorting of dried figs. It principally consists of three functioning elements: supply unit;
196 inspection unit and separation unit (figure 1).



197
198 *Figure 1. Picture of the in-line sorting prototype*

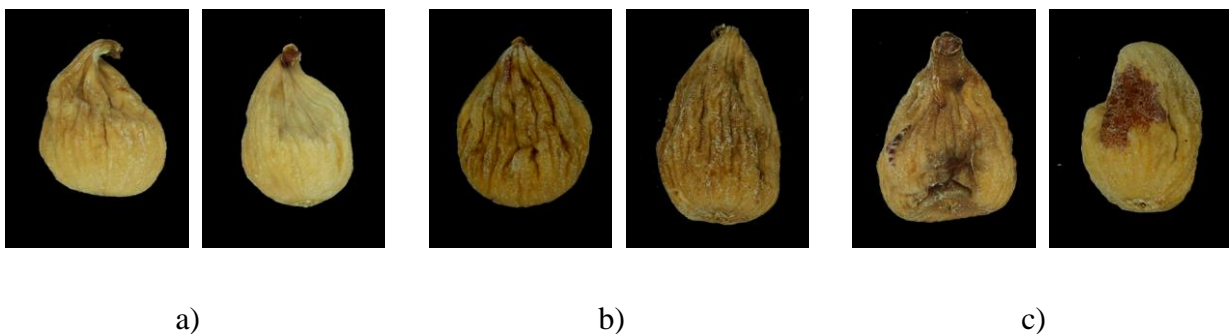
199 From the supply unit, fruit are spread on a number of conveyor belts, 30 mm wide and 250
200 mm long, moving at a relatively high speed (0.5 m/s). They pass through the inspection unit
201 which consists of two progressive scanning colour cameras (JAI CV-M77), placed at
202 approximately 0.9 m above the subject, which provide RGB images (512 x 384 pixels) with a
203 resolution of 0.70 mm/pixel. Cameras are equipped with a 12 mm lens, and lighting is
204 provided by light emitting diode (LED) lamps. The entire system is housed in a frame of
205 stainless steel suitable for agro-food products. After each image processing, the computer
206 responsible sends the following data: fruit position, the number of the conveyor belt on which
207 it is located, and the corresponding category to a second computer which is responsible for

208 directing the movement of the inspected fruit to the separation unit and its subsequent
209 categorisation.

210 A set of 24 figs was used to build the models and train the image processing software. This
211 was done by manually dividing the figs into the three different categories and passing each
212 category separately through the in-line prototype. The trials considered 96 figs, which had
213 previously been classified in the subsequent three categories: 31 light PDO figs, 26 dark PDO
214 figs and 39 deteriorated figs (figure 2). Each fruit in the validation set went through the whole
215 classification process five times in random positions, and orientations and sides, thus it was as
216 if 480 figs were categorised.

217 One of the requirements of current quality standards for dried figs is that the contents of each
218 package must be uniform (United Nations, 2014). Moreover, consumers are prone to purchase
219 lots with uniformity of colours and sizes. Hence, the output of each category was established
220 as follows:

- 221 • Category 0: (Light PDO figs): the fig arrives at the end of the conveyor belt.
- 222 • Category 1: (Dark PDO figs): the fig is ejected at the first outlet.
- 223 • Category 2: (Deteriorated figs): the fig is ejected at the second outlet.



224 Figure 2. Samples with different colours that belong to different categories: a) light, b) dark and c)
225 deteriorated uneven coloured figs

226 In-line systems working in real-time have to run very fast image processing algorithms and
227 hence it is not possible to incorporate complex segmentation models although it could be
228 more effective in some cases. On the other hand, it is very important that the quality
229 parameters can be easily controlled by non-experienced workers through a friendly interface.
230 This means that the machine has to prioritize easy to handle methods to separate the fruits
231 over other maybe more robust but also more complex statistical methods.

232 Following this principle, image segmentation was developed based on the colour analysis of
233 images captured with the aforementioned industrial cameras under dynamic conditions. As a
234 first step, each pixel in the image was classified as background or as belonging to an object to
235 be analysed. Since there was a marked contrast between the white background and the fruit, a
236 threshold was enough to properly remove the background from the image analysis.

237 Preliminary analysis of the histogram of the training images determined that a threshold value
238 of $T_0=100$ in the green band could separate the fruit without error. Therefore, any pixel with a
239 value in the G channel above T_0 could be considered as belonging to the background and
240 removed. This operation was performed only in the regions of interest corresponding to the
241 conveyor belts while the parts of the images outside these regions were not considered.

242 All remaining pixels in the images were considered as belonging to potential figs. Therefore,
243 the RGB values of the remaining pixels were converted into CIE XYZ and CIELAB
244 coordinates to calculate the *BI*.

245 To separate the pixels in the figs into any of the predefined classes a previous analysis was
246 necessary. An analysis of the variance (ANOVA) was carried out for each variable using the
247 training calibration samples to determine into which of the different available colour
248 coordinates the figs belonging to different qualities could be best placed, or if necessary, a
249 combination of several colour coordinates. Once the variables had been defined, the

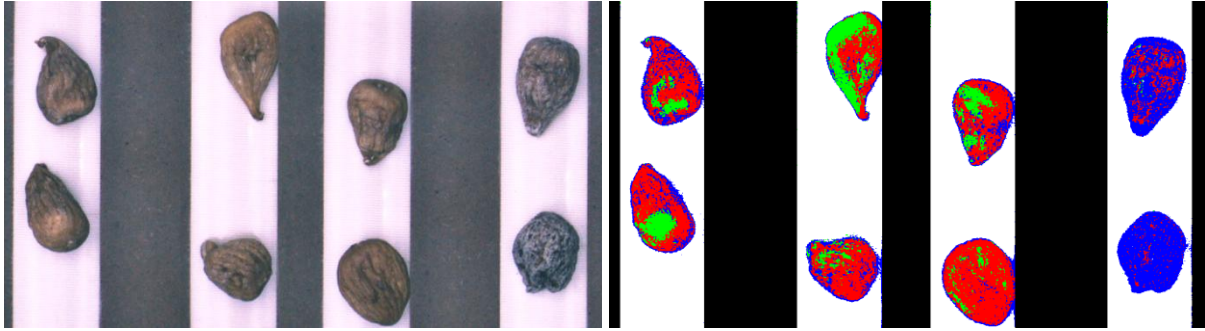
250 thresholds among the three classes initially set in the sorting prototype could be established
251 from the data extracted from the basic statistics (tables 3 and 4). Once the colour indices and
252 the thresholds had been determined, the algorithms were programmed to classify the pixels in
253 the images in one of the three categories as follows, where the thresholds T_1 and T_2 were
254 obtained from the previous analysis:

- 255 • If average $BI < T_1$ the pixel was considered deteriorated
- 256 • If average $BI \geq T_1$ and average $XYZ.X < T_2$, the pixel was considered a dark PDO;
257 otherwise the pixel was considered as belonging to a fair PDO fig.

258 After the pixelwise image segmentation, it was necessary to perform a filtering process in
259 order to reduce the noise caused by shadows found at the edges of the fig and by small groups
260 of isolated pixels. This process consisted of a two-iteration erosion of the complete fig
261 followed by a median filter. Finally, the categorisation of the fig was based on the class of
262 pixel which covered the largest part of the fig.

263 The sequence of image processing carried out by the sorting machine in real time is shown in
264 figure 3. The original image captured by the cameras shows the figs while they are
265 transported by the conveyor belts. The first step corresponds to the segmentation based on the
266 thresholds in the regions of interest defined by the known position of the conveyor belts. Then
267 the filtering is performed in order to reduce the noise and the segmentation problems caused
268 by shadows found at the edges of the figs. Finally, the decision is taken by counting the
269 number of pixels belonging to the different classes. For the case shown in figure 3, according
270 to the decision of the vision system, the figs in blue belong to the deteriorated class, the figs in
271 red are dark figs, and the fig in green is a light one.

272

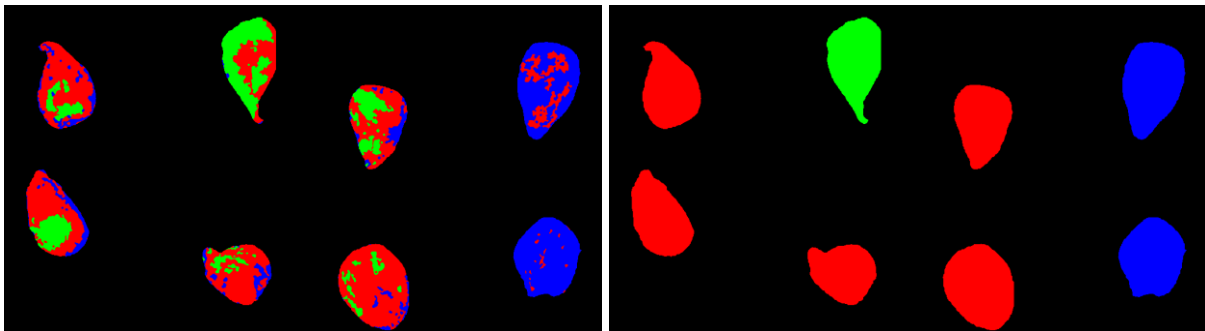


273

a)

b)

274



275

c)

d)

276 Figure 3. Steps in the in-line image processing of the figs sorting machine. a) original image captured
277 by the cameras, b) segmented image, c) filtered image, and d) decision image

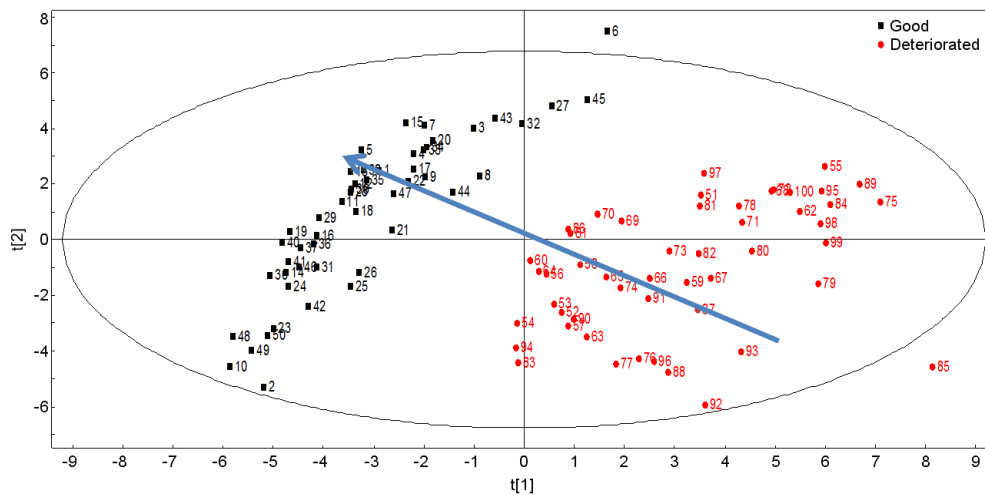
278 The tests were carried out by placing the figs into a vibrating platform that guided the fruit
279 randomly to the different conveyor belts of the prototype. Each fruit was transported by the
280 conveyor belts, analysed and sorted by the outlet corresponding to their assigned category.

281 3 RESULTS AND DISCUSSION

282 3.1. Dried Fig colour assessment

283 Figure 4 represents the score plot of PCA (2 PC's, R^2 81%), showing an overview of the
284 behaviour of each fruit belonging to the studied groups with PDO figs of Cosenza in black
285 and deteriorated ones in red. Here, as stated above, the analysis considered the totality of
286 variables (26), that is, those obtained by conventional colourimetry as well as those obtained

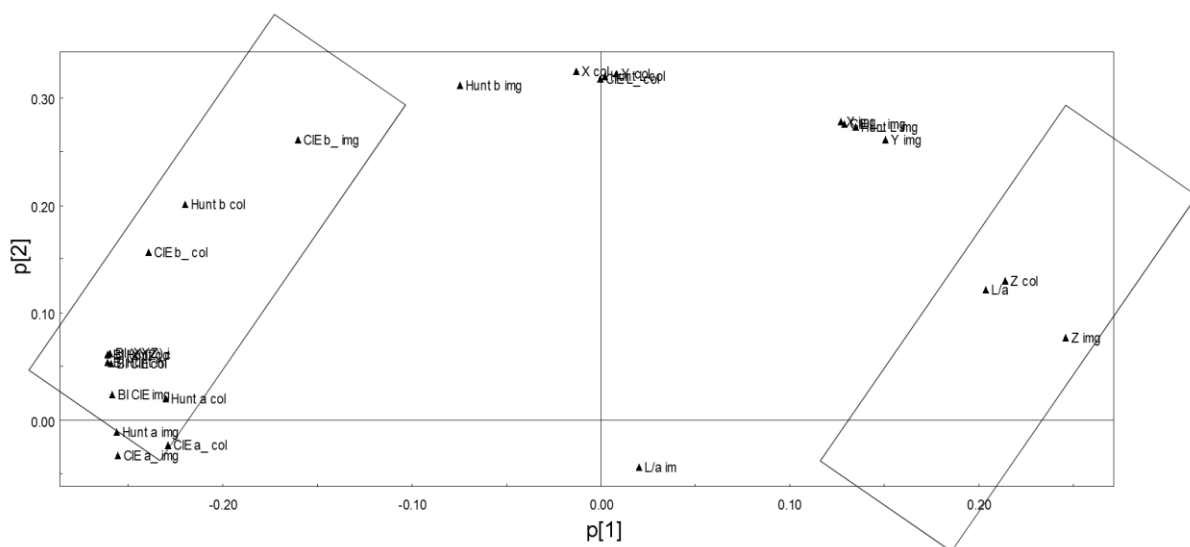
287 from image processing. In this case, the PCA model is able to separate the two classes. In
 288 order to assess for which components are mainly responsible for separation, the loadings plot
 289 (figure 5) is inspected.



290

291 Figure 4. Score plot of PCA results considering all the variables (image analysis and conventional
 292 colourimetry). The ellipse represents 95% confidence interval.

293 The separation between class 1 (sound figs represented by black points) and class 2
 294 (deteriorated figs represented by red points) is mainly characterized by the variables
 295 XYZ.Zcol, XYZ.Zimg and L/a on one hand, and CIEb_img, Huntb_col, and CIEb_col, on the
 296 other hand.

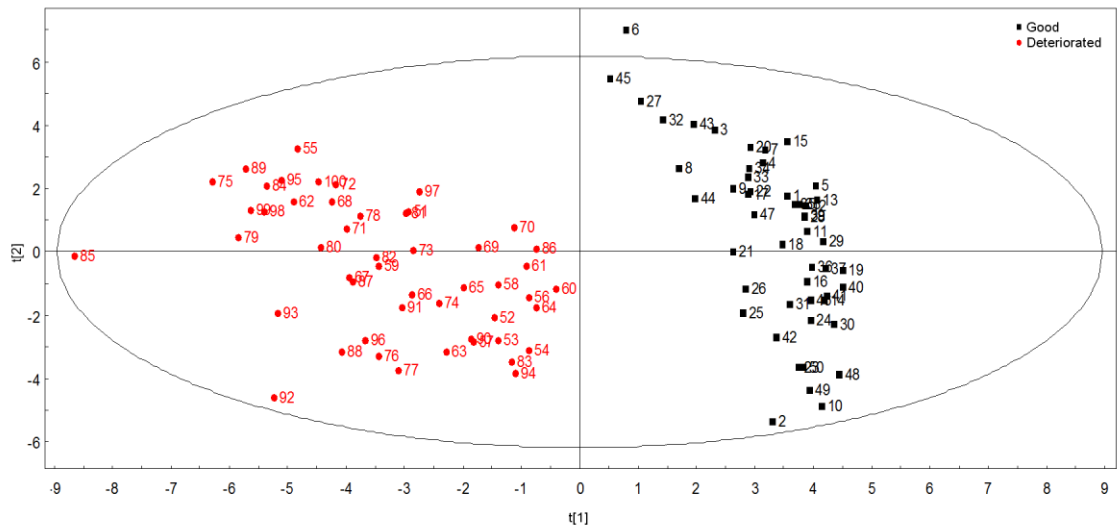


297

298 Figure 5. *Loading plot of PCA results considering all the variables (image analysis and conventional*
299 *colourimetry). The rectangles include the best separating variables.*

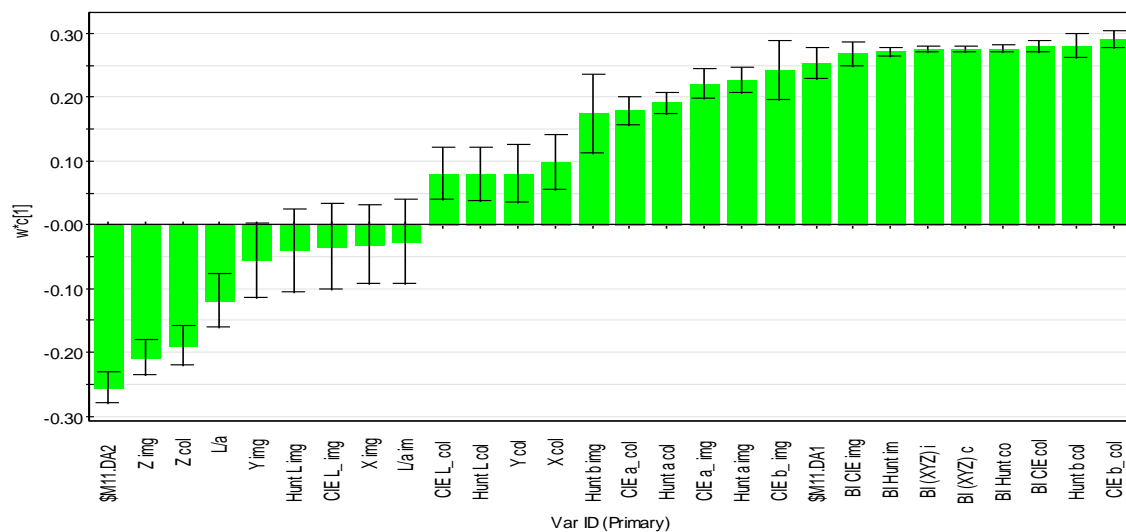
300 PLS-DA results highlight two clusters, each one corresponding to one of the assessed groups
301 of figs (figure 6). The plot shows that the first component is able to separate the two classes.
302 From the PLS-DA weights of the first component (figure 7), the variables responsible for the
303 separation can be derived. Note that, in the case of having more than one discriminant
304 component in the model, other approaches (e.g. VIP's) would be more sensitive.
305 Nevertheless, in this case, since the discriminant direction is mainly related to the first latent
306 variable, both approaches provide equivalent results (see figure 8), with the advantage that the
307 weights provide the positive or negative correlation of each variable with each of the classes
308 to be separated. It must be stated that, for classification purposes, the model was built with 5
309 latent variables and an R²Y value of 96.5% and a Q²Y value of 95%, which in practice
310 means that all figs were correctly classified in a 7-block cross-validation procedure. However,
311 this was not the goal of the analysis: the goal of the analysis being the selection of the most
312 discriminant variables and comparing them with the ones used in the already built in-line
313 sorting machine.

314 On the other hand, the score plots of PCA and PLS-DA show similar clusters for the two
315 studied groups, and PCA confirms that the XYZ.Z coordinate is one of the best discriminant
316 variables. The difference between the two score plots lies in the fact that PCA function is not
317 to separate both classes, but to maximise the variance, as previously stated. Anyway, since the
318 rotation in the components is not very large, the variables indicated by the loadings barplot
319 (figure 9) are almost the same as the ones outlined by the first component weights of the PLS-
320 DA model (figure 7).



321

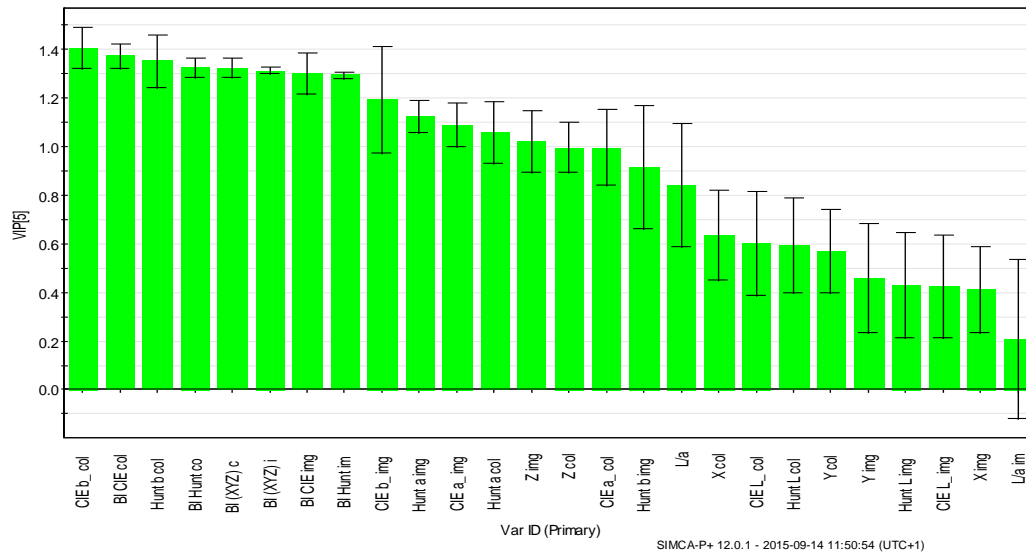
322 Figure 6. Score plot of PLS-DA results considering all the variables (image analysis and conventional
 323 colourimetry). The ellipse represents 95% confidence interval.



R2X[1] = 0.513287 SIMCA-P+ 12.0.1 - 2015-09-14 11:52:45 (UTC+1)

324

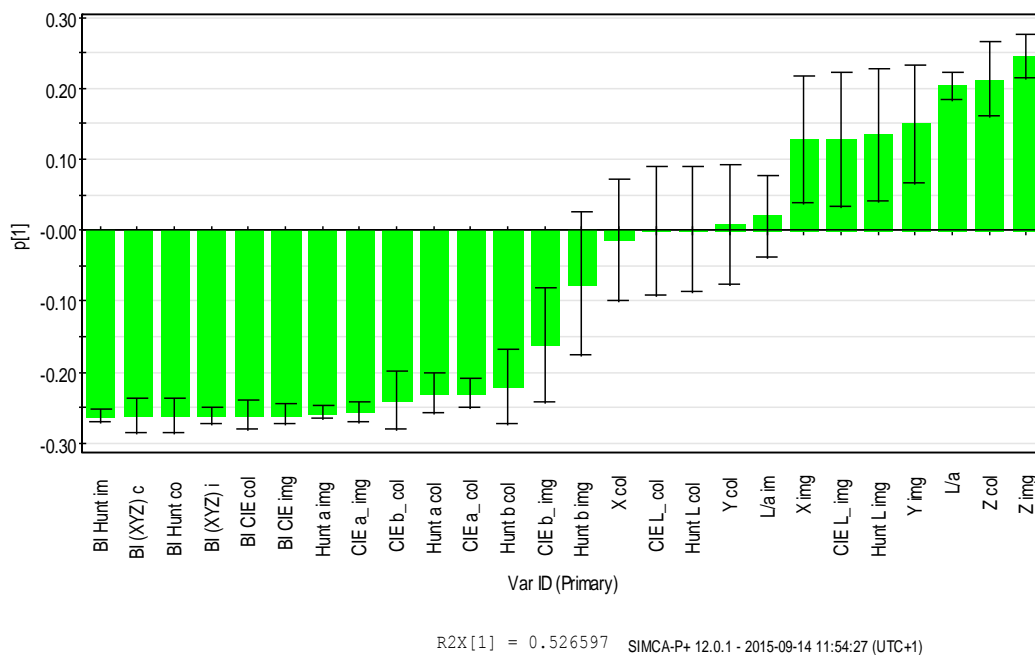
325 Figure 7. Weight plot of the first component of the PLS-DA model considering all the variables
 326 (image analysis and conventional colourimetry)



327

328 Figure 8. *VIP's plot of the first component of the PLS-DA model considering all the variables*

329 *(image analysis and conventional colourimetry)*



330

331 Figure 9. *Column plot of PCA for the first component considering all the variables (image analysis*

332 *and conventional colourimetry)*

333 The study carried out highlights that, in this case, both statistical analyses, PCA and PLS-DA,

334 could distinguish clearly between high quality PDO figs and deteriorated ones, showing the

335 effectiveness of both techniques used for fig colour assessment as a qualitative parameter.

336 Hence, analysis of high quality images could perfectly replace current destructive methods

337 based on sampling for this purpose. The browning index seemed to be an interesting index
 338 that showed this distinction, and therefore a valid indicator for dried fig quality assessment
 339 but the colour measurement in some different colour spaces did not present significant
 340 differences. It is important to consider all components in the model, and not only the first, to
 341 determine which indicate the discriminant direction (Prats-Montalbán et al., 2006).

342 **3.2. In-line dried fig sorting**

343 The methods, conditions, aims and equipment used for classifying the fruit in real-time using
 344 an industrial machine are different from those used to assess colour using a standard
 345 colourimeter and hence new variables need to be selected. ANOVAs carried out on the main
 346 discriminant variables highlighted by the PLS-DA and PCA analyses achieved similar results
 347 in terms of significance. From these analyses, variables *BI* and *X* were selected for separating
 348 the different categories of figs during the in-line real-time inspection using the machine since
 349 the study of the basic statistics clearly determined that it was possible to set thresholds to
 350 separate the different categories. Tables 1 and 2 show the ANOVA for these variables while
 351 tables 3 and 4 show the summary of the statistics. Browning index could be clearly used to
 352 separate between good and deteriorated figs and it was decided from these data to use a
 353 threshold value of $T_1=35$. On the other hand, dark and light figs could be separated using the
 354 *X* colour value and hence, using the data in table 4, a threshold value of $T_2=7$ was configured
 355 in the machine.

356 Table 1. Analysis of variance for Browning Index

<i>Source</i>	<i>Sum of Squares</i>	<i>Df</i>	<i>Mean Square</i>	<i>F-Ratio</i>	<i>P-Value</i>
Between groups	9435.52	2	4717.76	83.03	0.0000
Within groups	5284.36	93	56.82		
Total (Corr.)	14719.90	95			

357

358 Table 2. Analysis of variance for *X*

<i>Source</i>	<i>Sum of Squares</i>	<i>Df</i>	<i>Mean Square</i>	<i>F-Ratio</i>	<i>P-Value</i>
Between groups	311.73	2	155.86	53.48	0.0000
Within groups	271.04	93	2.91		
Total (Corr.)	582.77	95			

359

360 Table 3. Summary Statistics for Browning Index

<i>Class</i>	<i>Average</i>	<i>Standard deviation</i>	<i>Coeff. of variation</i>	<i>Min</i>	<i>Max</i>
Light	48.27	5.43	11.24%	36.58	59.54
Dark	43.13	8.43	19.90%	31.56	61.71
Deteriorated	25.93	8.31	32.04%	8.48	41.70

361

362 Table 4. Summary Statistics for *X*

<i>Class</i>	<i>Average</i>	<i>Standard deviation</i>	<i>Coeff. of variation</i>	<i>Min</i>	<i>Max</i>
Light	8.81	1.89	21.78%	6.32	14.53
Dark	5.63	0.90	15.90%	4.08	7.75
Deteriorated	10.08	1.94	19.26%	5.56	13.15

363

364 Results of the performance of the machine are shown in table 5. At the end of the trials,
 365 99.5% of deteriorated figs were correctly classified, as well as 89% of light PDO figs;
 366 however, just 69.2% of accurate classification was reached for dark PDO figs. This decrease
 367 of accuracy is related to the unevenness of the figs' skin colour. In fact, some fruits had a
 368 lighter colour on one side than on the other; consequently, the machine classified them
 369 according to the colour of the side showing as they randomly passed. It has to be remarked
 370 that the results correspond to the inspection of the validation set of the figs five times, but

371 each time they fall randomly onto the conveyor belts and were captured in a different and
372 random location in the image. This means that for each time, the conditions and lighting of
373 each particular fig were different.

374 A certain degree of confusion is normal using the fast classification method implemented.
375 However, the main confusion occurred between the light and dark figs which could be
376 acceptable since both are good quality figs separated only for commercial reasons. On the
377 other hand, there was little confusion between good and deteriorated figs, which is more
378 important from the point of view of the final quality. An aspect to improve is that the machine
379 classified 3.8% deteriorated figs as dark, which, even though within a 5% tolerance, should be
380 reduced. On the contrary, it would be of less importance if dark figs were classified as
381 deteriorated. These results illustrate that fig sorting, using the above-described system, was
382 achieved successfully. The highest percentage was obtained each time for deteriorated figs,
383 followed by light PDO ones, and then dark PDO figs.

384 Table 5. Results of automated sorting

Machine\Vis	Light PDO figs	Dark PDO figs	Deteriorated figs
Light PDO figs	89.0%	26.9%	0.5%
Dark PDO figs	11.0%	69.2%	0.0%
Deteriorate figs	0.0%	3.8%	99.5%

385

386 To identify a specific index to determine accurately the quality for PDO dried figs of
387 Cosenza, the achieved analysis has to be consolidated by further research, taking into account
388 additional parameters i.e., colour change according to ripeness, drying status as well as the
389 correlation of skin colour with anthocyanin content (Rodov et al., 2012). This may be

390 achieved and incorporated in the future to the in-line sorting machine with the use of faster
391 computing units.

392 Some of the problems found could be resolved using, instead of conveyer belts, bi-conic roller
393 conveyors (ElMasry et al., 2012) which turn the fruits as they progress, allowing the system to
394 inspect their whole surface. However, although a complex analysis of the colour or the texture
395 of the figs would result in a better accuracy of the classification, the computing requirements
396 would not ensure actual real-time processing at a commercial speed.

397 Image processing time was about 15 ms, permitting an analysis of up to 65 images/s.

398 However, due to mechanical limitations of the prototype, and also because a very high speed
399 could damage the product when it is expelled by the outlets, the speed of the conveyor belts
400 was limited to 0.5 m/s, obtaining then 10 analysed images per second. Considering an ideal
401 distance of 0.1 m between two consecutive figs, at the highest speed of the conveyor belts
402 (0.5 m/s), the tested prototype has the productivity of about 40 figs/s, corresponding
403 approximately to 2160 kg/hour. The system has been tested on a prototype with several
404 mechanical limitations, and it is expected that the performance in terms of accuracy and
405 capacity of fruit processing will be higher when the system is developed industrially.

406 **4 CONCLUSIONS**

407 As currently carried out, dried fig inspection and grading methods are labour intensive and
408 unreliable due to machine speed and inspector fatigue. Therefore, the development of an
409 effective integrated inspection system that can detect quality according to previously
410 established parameters of the whole fruit would be valuable for the fig industry. The present
411 work showed that the combination of computer vision systems and latent-based multivariate
412 statistical projection models used for this purpose allowed these objectives to be reached
413 under laboratory conditions for manual quality inspection which can be suitable for small-

414 scale production or when the control of only a limited number of samples is required. These
415 results are interesting because they illustrated that both chroma meter and image analysis
416 allowed an effective distinction between high quality dried figs and deteriorated ones, based
417 on colour parameters, a camera being much cheaper and easier to use than the chroma meter.
418 A system for in-line sorting of figs in real-time was developed based on computer vision and
419 colour parameters providing reliable results. This is the first attempt to create a machine
420 capable of sorting dried figs in real-time using computer vision and a machine with the
421 capability of separating the fruit into different categories. The system could classify correctly
422 between three classes of figs using the browning index and the *X* colour coordinate. The test
423 was carried out in dynamic conditions with the figs being transported under the camera at
424 high speed, and subsequently separating the figs into different categories by different outlets
425 depending on the decision of the vision system. This was repeated five times, each time
426 achieving good results, the major confusion being between the two classes of sound figs, but a
427 minimal confusion of only 0.5% was found between sound and deteriorated figs: this
428 distinction being the most important from the commercial point of view.

429 **Acknowledgement**

430 This work has been partially funded by INIA through research project RTA2012-00062-C04-
431 01 with the support of European FEDER funds.

432 *All authors contributed equally to the present work.*

433 **5 REFERENCES**

434 Benalia, S., Bernardi, B., Cubero, S., Leuzzi, A., Larizza, M., & Blasco, J. (2015).
435 Preliminary trials on Hyperspectral Imaging Implementation to Detect Mycotoxins in Dried
436 Figs. *Chemical Engineering Transaction*, 44, 157- 162. doi: 10.3303/CET1544027

437 Blasco, J., Aleixos, N., Cubero, S., Gómez-Sanchís, J., & Moltó, E. (2009a). Automatic
438 sorting of satsuma (*Citrus unshiu*) segments using computer vision and morphological
439 features. *Computers and Electronics in Agriculture*, 66(1), 1–8.
440 doi:10.1016/j.compag.2008.11.006

441 Blasco, J., Cubero, S., Gómez-Sanchís, J., Mira, P., & Moltó, E. (2009b). Development of a
442 machine for the automatic sorting of pomegranate (*Punica granatum*) arils based on computer
443 vision. *Journal of Food Engineering*, 90(1), 27–34. doi:10.1016/j.jfoodeng.2008.05.035

444 Cubero, S., Aleixos, N., Moltó, E., Gómez-Sanchis, J., & Blasco, J. (2011). Advances in
445 Machine Vision Applications for Automatic Inspection and Quality Evaluation of Fruits and
446 Vegetables. *Food and Bioprocess Technology*, 4(4), 487–504. doi:10.1007/s11947-010-0411-
447 8

448 De Luca, A.I., Molari, G., Seddaiu, G., Toscano, A., Bombino, G., Ledda, L., Milani, M.,
449 Vittuari, M. (2015b). Multidisciplinary and innovative methodologies for sustainable
450 management in agricultural systems. *Environmental Engineering and Management Journal*,
451 14 (7), 1571-1581.

452 Elmasry, G., Cubero, S., Moltó, E., & Blasco, J. (2012). In-line sorting of irregular potatoes
453 by using automated computer-based machine vision system. *Journal of Food Engineering*,
454 112(1-2), 60–68. doi:10.1016/j.jfoodeng.2012.03.027

455 European Commission. (1996). Commission approves the registration of agricultural and food
456 products. Retrieved from http://europa.eu/rapid/press-release_IP-96-492_en.htm

457 European Commission. (2011). Commission Implementing Regulation (EU) No 596/2011 of
458 7 June 2011 entering a name in the register of protected designations of origin and protected

459 geographical indications [Fichi di Cosenza (PDO)]. OJ L 162, 22/06/2011, 1–2. Retrieved
460 from <http://eur-lex.europa.eu/legal-content/EN/TXT/PDF/?uri=CELEX:32011R0596&rid=4>

461 Farahnaky, A., Ansari, S., & Majzoobi, M. (2009). Effect of glycerol on the moisture sorption
462 isotherms of figs. *Journal of Food Engineering*, 93(4), 468–473.
463 doi:10.1016/j.jfoodeng.2009.02.014

464 Geladi, P., Kowalski, B.R. (1986). Partial Least-Squares Regression: A Tutorial. *Analytica*
465 *Chimica Acta*, 185, 1-17.

466 Gómez-Sanchis, J., Blasco, J., Soria-Olivas, E., Lorente, D., Escandell-Montero, P., Martínez-
467 Martínez, J. M., Aleixos, N. (2013). Hyperspectral LCTF-based system for classification of
468 decay in mandarins caused by *Penicillium digitatum* and *Penicillium italicum* using the most
469 relevant bands and non-linear classifiers. *Postharvest Biology and Technology*, 82, 76–86.
470 doi:10.1016/j.postharvbio.2013.02.011

471 González-Miret, M. L., Ayala, F., Terrab, A., Echávarri, J. F., Negueruela, a. I., & Heredia, F.
472 J. (2007). Simplified method for calculating colour of honey by application of the
473 characteristic vector method. *Food Research International*, 40(8), 1080–1086.
474 doi:10.1016/j.foodres.2007.06.001

475 Grahn, H. F., & Geladi, P. (2007). Techniques and Applications of Hyperspectral Image
476 Analysis. John Wiley & Sons, Ed., vol. 22. doi:10.1002/9780470010884

477 Hatano, K., Kubota, K., & Tanokura, M. (2008). Investigation of chemical structure of non
478 protein proteinase inhibitors from dried figs. *Food Chemistry*, 107(1), 305–311.
479 doi:10.1016/j.foodchem.2007.08.029

480 HunterLab. (2008). Applications note, 8(9), available at: [https://support.hunterlab.com/hc/en-](https://support.hunterlab.com/hc/en-us/articles/203997085-Hunter-L-a-b-Colour-Scale-an08-96a)
481 [us/articles/203997085-Hunter-L-a-b-Colour-Scale-an08-96a](https://support.hunterlab.com/hc/en-us/articles/203997085-Hunter-L-a-b-Colour-Scale-an08-96a). Last accessed: August 2015.

482 IPGRI, & CIHEAM. (2003). Descriptors for fig. International Plant Genetic Resources
483 Institute, Rome, Italy, and International Centre for Advanced Mediterranean Agronomic
484 Studies, Paris, France. Retrieved from <http://www.ipgri.cgiar.org/>

485 Jackson, J.E. (1991). *A User's Guide to Principal Components*. New York: Wiley.

486 Kang, S. P. P., & Sabarez, H. T. T. (2009). Simple colour image segmentation of bicolour
487 food products for quality measurement. *Journal of Food Engineering*, 94(1), 21–25.
488 doi:10.1016/j.jfoodeng.2009.02.022

489 Martin, M. L. G.-M., Ji, W., Luo, R., Hutchings, J., & Heredia, F. J. (2007). Measuring colour
490 appearance of red wines. *Food Quality and Preference*, 18(6), 862–871.
491 doi:10.1016/j.foodqual.2007.01.013

492 Mendoza, F., Dejmek, P., & Aguilera, J. M. (2006). Calibrated colour measurements of
493 agricultural foods using image analysis. *Postharvest Biology and Technology*, 41(3), 285–
494 295. doi:10.1016/j.postharvbio.2006.04.004

495 Menesatti, P., Zanella, A., D'Andrea, S., Costa, C., Paglia, G., Pallottino, F. (2009).
496 Supervised multivariate analysis of hyper-spectral NIR images to evaluate the starch index of
497 apples. *Food and Bioprocess Technology*, 2(3), 308-314. DOI: 0.1007/s11947-008-0120-8

498 Menesatti, P., Angelini, C., Pallottino, F., Antonucci, F., Aguzzi, J., Costa, C. (2012) RGB
499 colour calibration for quantitative image analysis: The "3D Thin-Plate Spline" warping
500 approach. *Sensors*, 12, 7063-7079

501 Mohammad, A., Rafiee, S., Emam-Djomeh, Z., & Keyhani, A. (2008). Kinetic Models for
502 Colour Changes in Kiwifruit Slices During Hot Air Drying. *World Journal of Agricultural*
503 *Sciences*, 4(3), 376–383.

504 Pallottino, F., Costa, C., Antonucci, F., Menesatti, P. (2013). Sweet cherry freshness
505 evaluation through colourimetric and morphometric stem analysis: Two refrigeration systems
506 compared. *Acta Alimentaria*, 42, 428-436

507 Pallottino, F., Menesatti, P., Lanza, M.C., Strano, M.C., Antonucci, F., Moresi, M. (2013).
508 Assessment of quality-assured Tarocco orange fruit sorting rules by combined
509 physicochemical and sensory testing. *Journal of the Science of Food and Agriculture*, 93,
510 1176,1183 Palou, E., López-Malo, A., Barbosa-Cánovas, G. V, Welte-Chanes, J., & Swanson,
511 B. G. (1999). Polyphenoloxidase Activity and Colour of Blanched and High Hydrostatic
512 Pressure Treated Banana Puree. *Journal of Food Science*, 64(1), 42–45. doi:10.1111/j.1365-
513 2621.1999.tb09857.x

514 Prats-Montalbán, J. M., de Juan, A., & Ferrer, A. (2011). Multivariate image analysis: A
515 review with applications. *Chemometrics and Intelligent Laboratory Systems*, 107(1), 1–23.
516 doi:10.1016/j.chemolab.2011.03.002

517 Prats-Montalbán, J. M., Ferrer, A., Malo, J. L., & Gorbeña, J. (2006). A comparison of
518 different discriminant analysis techniques in a steel industry welding process. *Chemometrics
519 and Intelligent Laboratory Systems*, 80(1), 109–119. doi:10.1016/j.chemolab.2005.08.005

520 Rodov, V., Vinokur, Y., & Horev, B. (2012). Brief postharvest exposure to pulsed light
521 stimulates colouration and anthocyanin accumulation in fig fruit (*Ficus carica* L.).
522 *Postharvest Biology and Technology*, 68, 43–46. doi:10.1016/j.postharvbio.2012.02.001

523 Sjöström, M., Wold, S., Söderström B. (1985). PLS discriminant plots. *Proceedings of PARC
524 in Practice*, Amsterdam, June 19– 21. North-Holland: Elsevier Science Publishers B.V.

525 United Nations. (2014). Recommendation on trial through 2014 for UNECE STANDARD
526 DDP- concerning the marketing and 2013 EDITION.

527 Valadez-Blanco, R., Viridi, a. I. S., Balke, S. T., & Diosady, L. L. (2007). In-line colour
528 monitoring during food extrusion: Sensitivity and correlation with product colour. *Food*
529 *Research International*, 40(9), 1129–1139. doi:10.1016/j.foodres.2007.06.008

530 Vallejo, F., Marín, J. G., & Tomás-Barberán, F. A. (2012). Phenolic compound content of
531 fresh and dried figs (*Ficus carica* L.). *Food Chemistry*, 130(3), 485–492.
532 doi:10.1016/j.foodchem.2011.07.032

533 Vidal, A., Talens, P., Prats-Montalbán, J. M., Cubero, S., Albert, F., & Blasco, J. (2013). In-
534 Line Estimation of the Standard Colour Index of Citrus Fruits Using a Computer Vision
535 System Developed For a Mobile Platform. *Food and Bioprocess Technology*, 6(12), 3412–
536 3419. doi:10.1007/s11947-012-1015-2

537 **Web references**

538 [http://agri.istat.it/sag_is_pdwout/jsp/dawinci.jsp?q=plC190000010000032100&an=2013&ig=](http://agri.istat.it/sag_is_pdwout/jsp/dawinci.jsp?q=plC190000010000032100&an=2013&ig=1&ct=270&id=15A|21A|30A)
539 [1&ct=270&id=15A|21A|30A](http://agri.istat.it/sag_is_pdwout/jsp/dawinci.jsp?q=plC190000010000032100&an=2013&ig=1&ct=270&id=15A|21A|30A) (accessed on March 31st, 2015)

540 <http://faostat3.fao.org/browse/Q/QC/E> (accessed on March 30th, 2015)

Table 1. Analysis of variance for Browning Index

<i>Source</i>	<i>Sum of Squares</i>	<i>Df</i>	<i>Mean Square</i>	<i>F-Ratio</i>	<i>P-Value</i>
Between groups	9435.52	2	4717.76	83.03	0.0000
Within groups	5284.36	93	56.82		
Total (Corr.)	14719.90	95			

Table 2. Analysis of variance for X

<i>Source</i>	<i>Sum of Squares</i>	<i>Df</i>	<i>Mean Square</i>	<i>F-Ratio</i>	<i>P-Value</i>
Between groups	311.73	2	155.86	53.48	0.0000
Within groups	271.04	93	2.91		
Total (Corr.)	582.77	95			

Table 3. Summary Statistics for Browning Index

<i>Class</i>	<i>Average</i>	<i>Standard deviation</i>	<i>Coeff. of variation</i>	<i>Min</i>	<i>Max</i>
Light	48.27	5.43	11.24%	36.58	59.54
Dark	43.13	8.43	19.90%	31.56	61.71
Deteriorated	25.93	8.31	32.04%	8.48	41.70

Table 4. Summary Statistics for X

<i>Class</i>	<i>Average</i>	<i>Standard deviation</i>	<i>Coeff. of variation</i>	<i>Min</i>	<i>Max</i>
Light	8.81	1.89	21.78%	6.32	14.53
Dark	5.63	0.90	15.90%	4.08	7.75
Deteriorated	10.08	1.94	19.26%	5.56	13.15

Table 5. Results of automated sorting

Machine\Vis	Light PDO figs	Dark PDO figs	Deteriorated figs
Light PDO figs	89.0%	26.9%	0.5%
Dark PDO figs	11.0%	69.2%	0.0%
Deteriorate figs	0.0%	3.8%	99.5%

Figure 1

[Click here to download high resolution image](#)

Figure 2 a1

[Click here to download high resolution image](#)

Figure 2 a2

[Click here to download high resolution image](#)

Figure 2 b1

[Click here to download high resolution image](#)

Figure 2 b2

[Click here to download high resolution image](#)

Figure 2 c1

[Click here to download high resolution image](#)

Figure 2 c2

[Click here to download high resolution image](#)

Figure 3a
[Click here to download high resolution image](#)



Figure 3b
[Click here to download high resolution image](#)

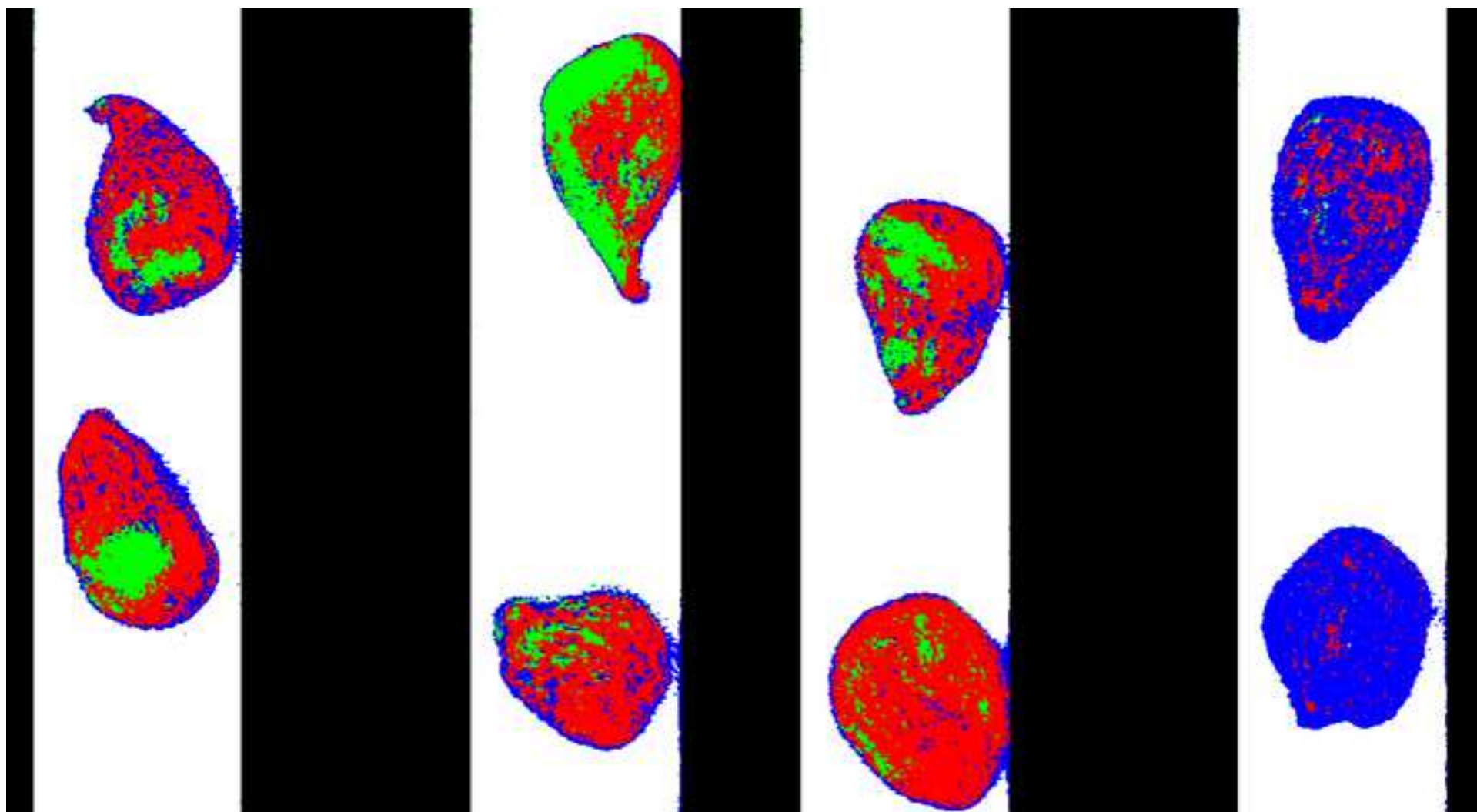


Figure 3c
[Click here to download high resolution image](#)

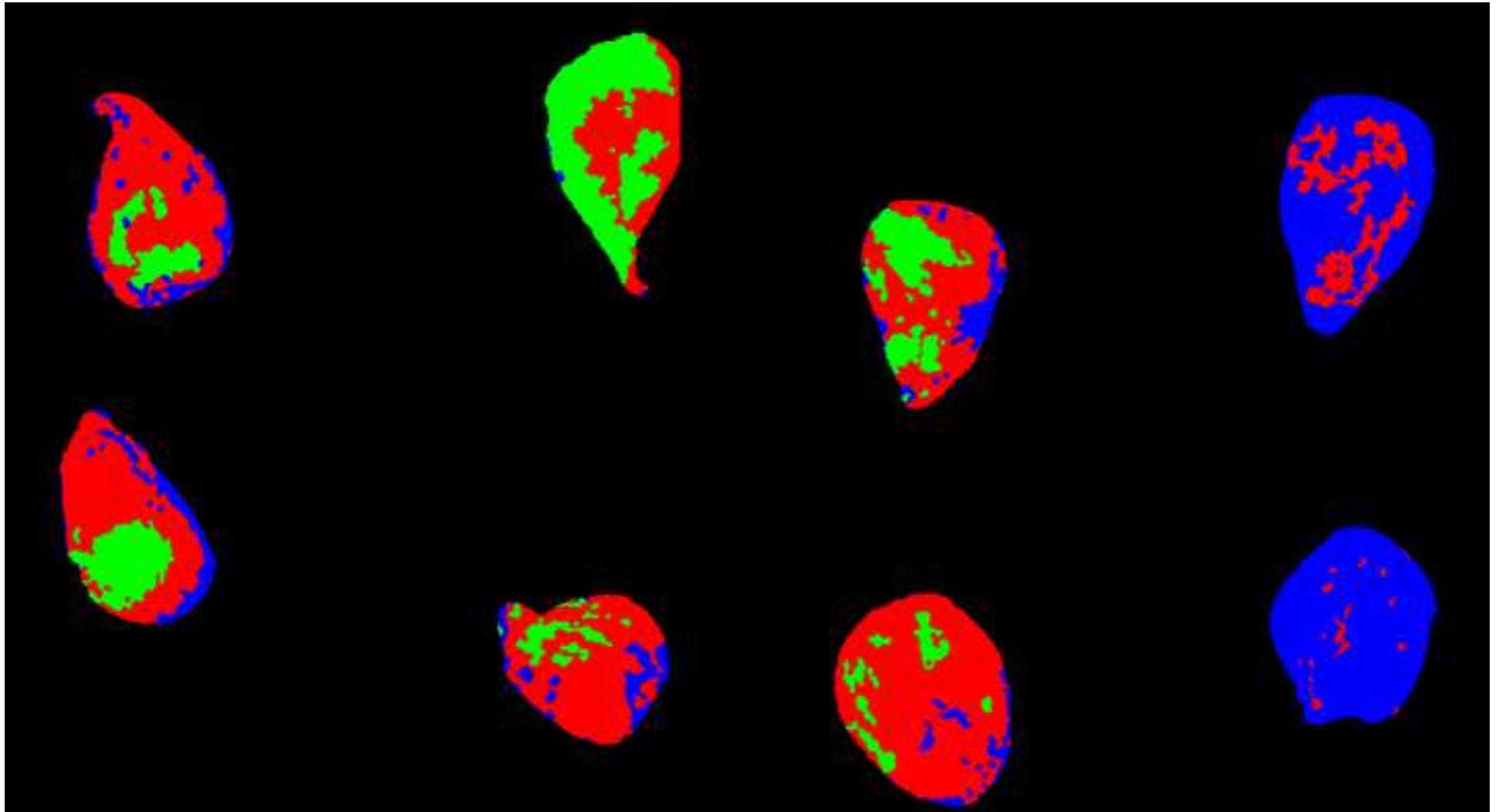


Figure 3d
[Click here to download high resolution image](#)

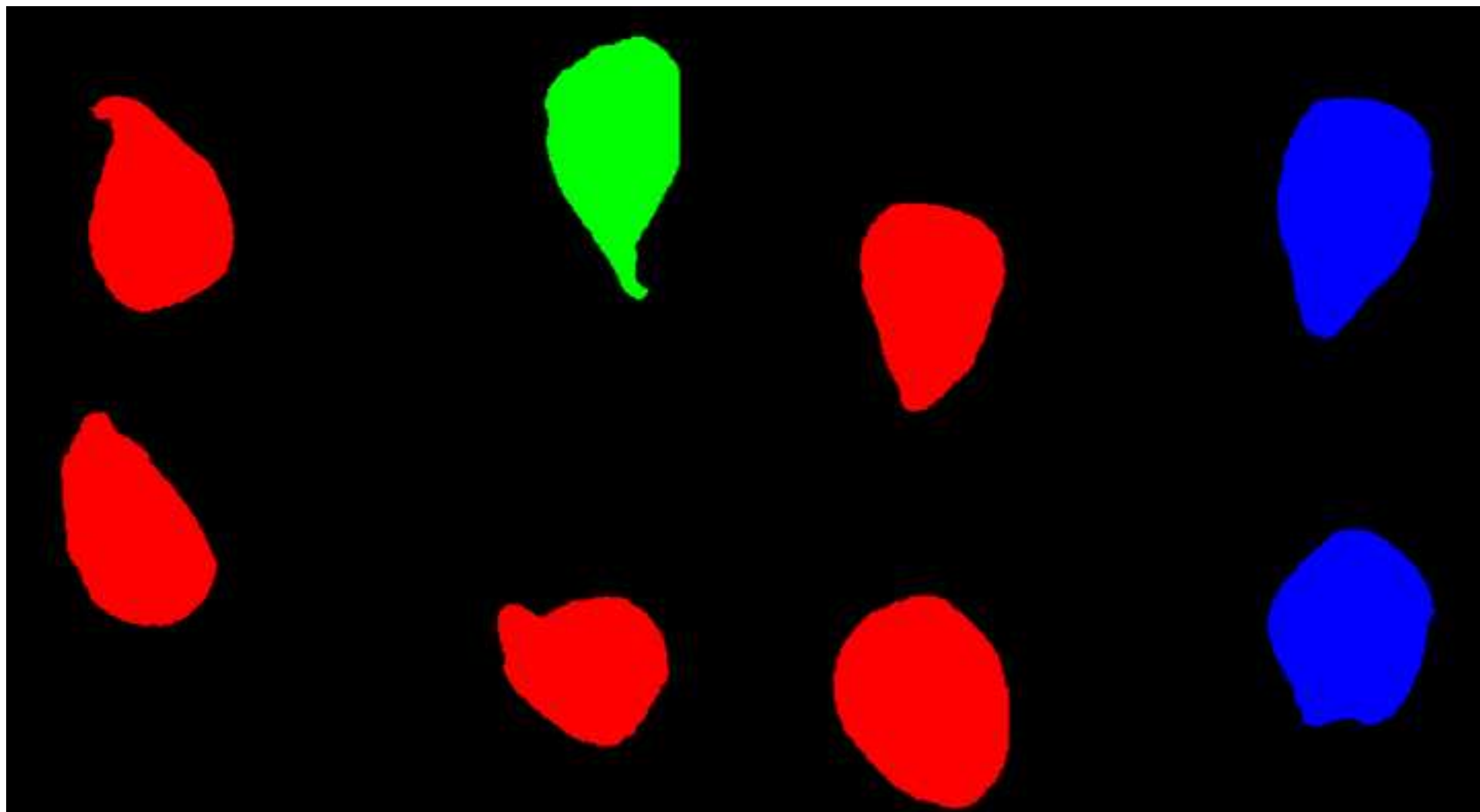


Figure 4
[Click here to download high resolution image](#)

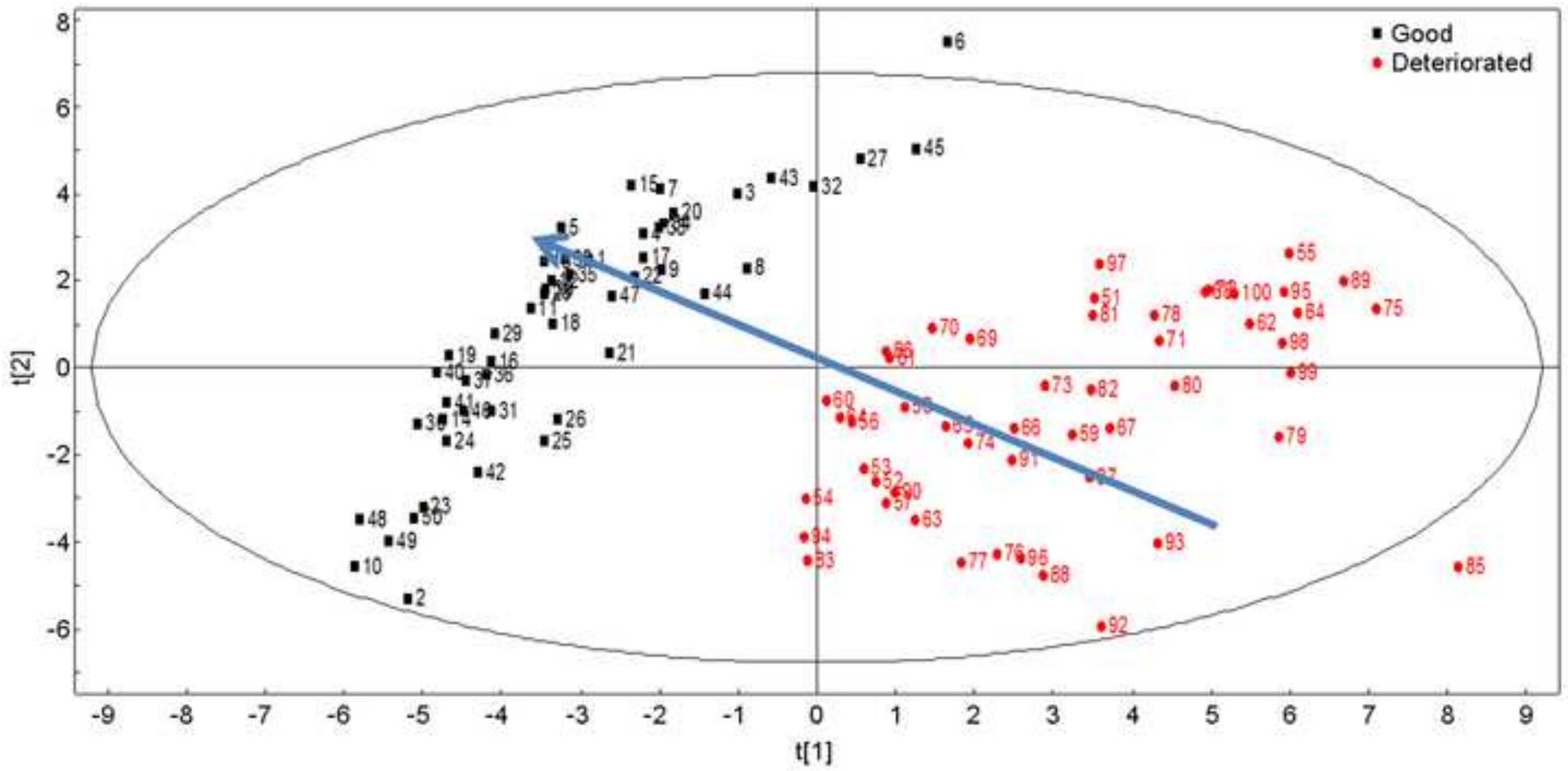


Figure 5
[Click here to download high resolution image](#)

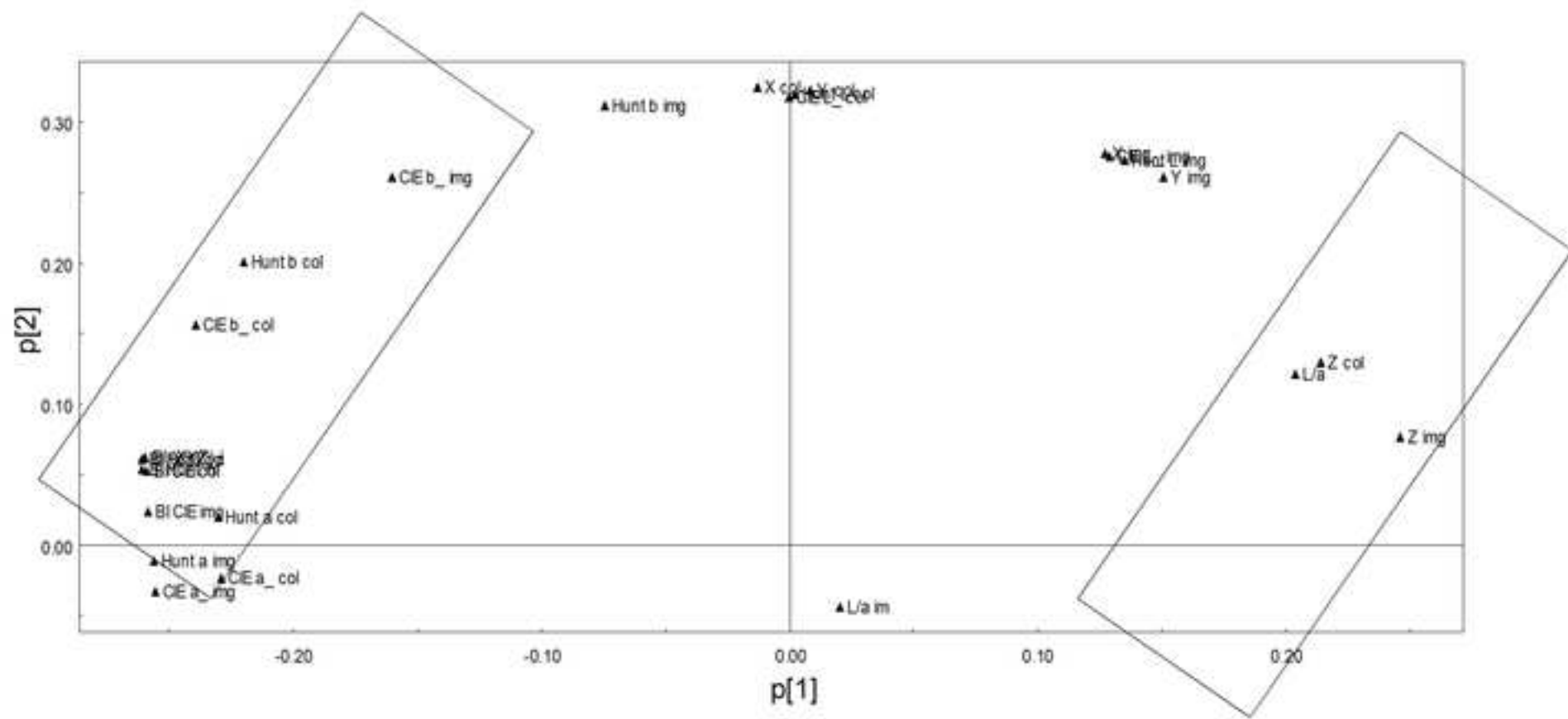


Figure 6
[Click here to download high resolution image](#)

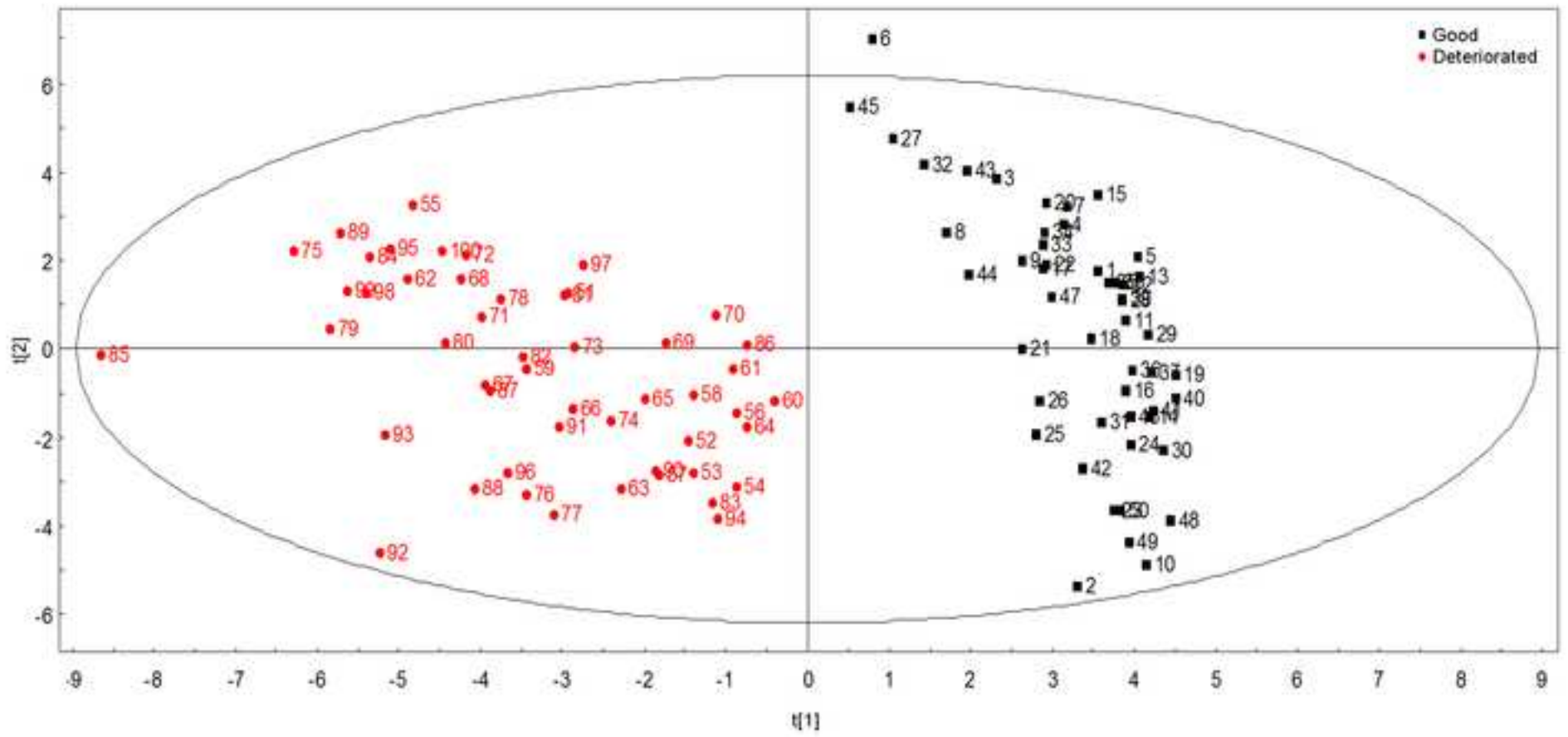


Figure 7

[Click here to download high resolution image](#)

Figure 8

[Click here to download high resolution image](#)

Figure 9

[Click here to download high resolution image](#)

Supplementary Material

[Click here to download Supplementary Material: Figures captions.docx](#)

<http://dx.doi.org/10.1016/j.compag.2015.11.002>